Failure process and stability analysis of landslides in Southwest China while considering rainfall and supporting conditions

Yaohui Gao[1], Yan Zhang[2]*, Chunchi Ma[2]*, Xiangsheng Zheng[2], Tianbin Li[2], Peng Zeng[2] and Juncheng Jin[3]

[1]PowerChina Huadong Engineering Corporation Limited, Hangzhou, China, [2]State Key Laboratory of Geohazard Prevention and Environment Protection, Chengdu University of Technology, Chengdu, China, [3]Chongqing 208 Geological Environment Research Institute Co., Ltd, Chongqing, China

Landslides frequently occur in several mountainous areas because of their unique engineering–geological conditions and other external factors (earthquakes, rainfall, etc.). In this paper, the landslide in Southwest China is used as the research objective to examine the landslide's stability under different working conditions. The influencing factors and the formation mechanism of the landslide are analyzed based on the geological environment and essential characteristics of the landslide. In addition, the transfer coefficient method and the GeoStudio software were used to assess the landslide stability. The analysis results demonstrate that the joint action of landforms, geological structures, rainfall, and other factors caused the landslide. Furthermore, the slipped tension fracture induced the failure mode. The transfer coefficient method results showed that the landslide was stable under natural conditions and unstable under rainstorm conditions, which is consistent with the numerical simulation result. The shear strength sensitivity analysis results depicted an apparent linear relationship among cohesion c, internal friction angle φ, and stability coefficient. Moreover, the stability of the unstable slope is more sensitive to φ than to c.

KEYWORDS

landslide, failure process, stability analysis, numerical simulation, transfer coefficient method

1 Introduction

Landslide refers to the sliding phenomenon of slope rock mass along the penetrating shear failure surface. China is one of the countries that face the world's most pervasive and severe landslide hazards (Fan et al., 2019; Tang et al., 2019; Gong et al., 2021; Luo et al., 2021). The landslides cause imbalance and destruction of the ecological environment and a variety of property losses and casualties, substantially impairing the local socio-

economic development. Therefore, it is crucial to investigate the formation mechanism and stability of landslides.

The principle of primary prevention and timely treatment is followed in the prevention and management of landslides. The most critical issue in landslide warning and treatment is assessing landslide stability. Numerous methods, such as the limit equilibrium method and numerical analysis method, can be used to study landslide's stability.

The limit equilibrium method is mainly based on theoretical calculation. Duncan (1996) reviewed the limit equilibrium method. Zhou et al. (2010) theoretically analyzed the limit equilibrium method by solving high-order equations. Based on the slice method, many scholars have assessed the stability of landslides with other knowledge (Chen et al., 2016; Guo et al., 2019). Xu et al. (2009) applied the shear strength reduction finite element method to examine the stability and potential failure mechanism of three landslides in the Huangla rock group upstream of the Three Gorges Dam. Zhou et al. (2019) investigated the stability of the circular slope at the foot of the slope using random field theory from the probability perspective and analyzed the relationship between the failure probability and the related length of the circular slope at the uniform foot of the slope. Sarkar et al. (2021) conducted a quantitative stability assessment *via* rock mass classification and finite element analysis. The cutting slope was divided into different risk grades according to the obtained stability grade and safety factor values. Although applying the limit equilibrium method provides more flexibility, there are still some limitations. Firstly, the deformation of the geological body was not considered, and the material is considered rigid. Second, the stress-strain relationship between rock and soil in the slope was also not considered. Third, the safety factor was only assumed to be the average safety factor on the slip surface.

Compared with the limit equilibrium method, the numerical analysis method is based on theoretical calculation and depends on the computer to calculate the landslide's stability. The stress-strain relationship of the rock and soil is obtained *via* computer processing while dealing with heterogeneous, non-linear, and complex boundary slopes. The excavation, support, and groundwater seepage of the slope can be simulated to analyze the interaction between the rock and soil and the supporting structure. With the advancements in computer technologies, some software, such as GEOSLOPE, FLAC^{3D}, ANSYS, among others, are used to calculate of landslides' stability. The finite element method, finite difference method, boundary element method, and discrete element method are some frequently used numerical calculation methods (Cheng et al., 2008; Zhao et al., 2020; Luo et al., 2021; Li et al., 2022). Some researchers have evaluated the stability of landslides based on these four methods. Zhao et al. (2020) applied a three-dimensional distance potential discrete element model to simulate the whole process of the Tangjiashan landslide movement. Tao et al. (2019) used the GEOSLOPE software to evaluate the effects of rock and soil parameters on the sensitivity of
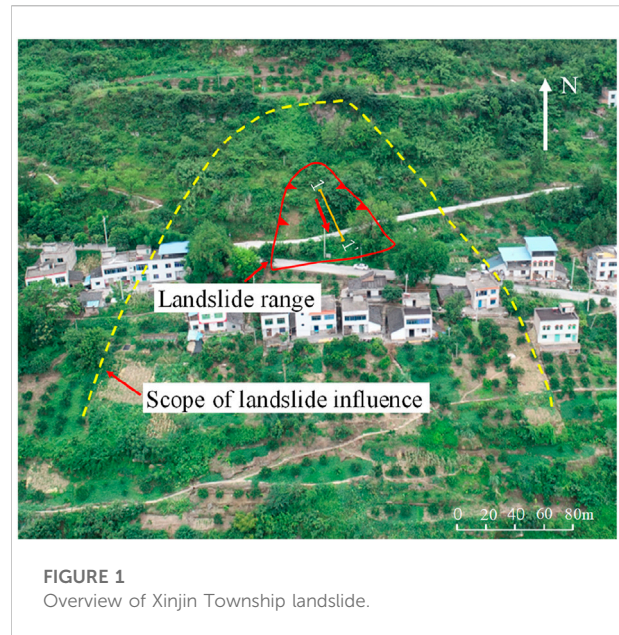
FIGURE 1
Overview of Xinjin Township landslide.

the Shimen landslide through a single characteristic factor analysis. Zhang et al. (2019) implemented GeoStudio software to select three factors, internal friction angle, cohesion, and rainfall, for an orthogonal test and used the range analysis method to assess the sensitivity of landslide's stability. Ma et al. (2021) examined the slope's stability using FLAC while considering the complex stress state, change in groundwater level, and seepage conditions.

This research uses the landslide in Xinjin Township, Yunyang County, as an example. It combines the collected regional data and the field survey results to analyze the deformation characteristics and formation mechanism of the landslide in Xinjin Township. The landslide's stability under different working conditions was calculated by the transfer coefficient method. Three limit equilibrium methods, Morgenstern-Price, Bishop, and Janbu, were further compared with the transfer coefficient method to investigate the landslide's stability through the GeoStudio software. The research results are valuable for the stability analysis of landslides under various working conditions.

2 Overview and cause analysis of landslide

2.1 Overview of a landslide

The landslide was situated in Xinjin Village, Xinjin Township, Yunyang County. It was about 40 m long in the longitudinal direction and 20–40-m wide in the transverse direction. The sliding body's thickness was 6.8–20.9 m, with an average thickness of about 14 m. The entire landslide's

FIGURE 2
Engineering–geological profile of the Xinjin Township landslide. (1−1′ profile in Figure 1).
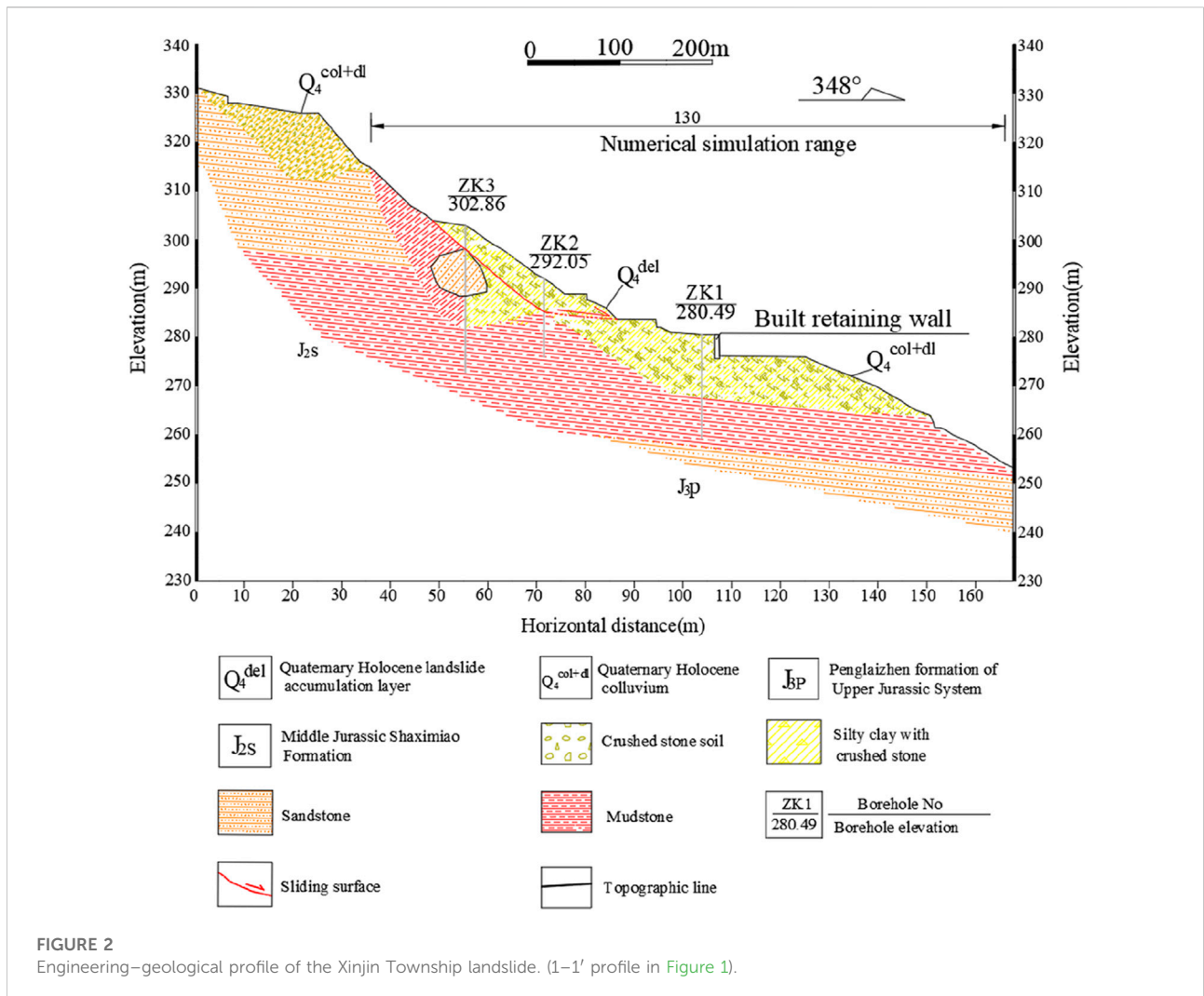
volume was approximately 1.7 m³ × 10⁴ m³, making it a small, medium-sized soil landslide. The landslide primarily threatens the safety of lives and properties of 22 households, more than 101 individuals, 240 m of county road, 140 m of the village road, pedestrians and vehicles, and the safety of rural road traffic, which may result in direct economic losses of around 14.313 million yuan. Figures 1, 2 illustrate the complete picture and the profile of the landslide, respectively.

2.1.1 Topography

The landslide area consists of tectonic denudation and the erosion of the low mountain slope landscape. It is situated on the right bank of the Yangtze river, encompassing the overall terrain of high south and low north. The landslide zone descends slowly, with a trailing edge and central slope angle of 30°–40°. The leading edge of the terrain slope angle has a ladder-like appearance, and the slope generally lies between 10° and 15°. The terrain slope in the

landslide area is typically slow-steep-slow. Surface vegetation, which is dominated mainly by shrubs, is present in this area.

2.1.2 Geological structure

The landslide area is located on the near axis of the southeast wing of the Wanzhou syncline. It has a monoclinic rock stratum, and the dominant rock stratum is at 350°∠6°. Bedrock fissures are also present in this area. The leading characteristics of the two groups of dominant fissures are as follows. LX1: 0°–20°∠81°–84°, relatively straight, opening width = 2–40 cm, extension = 3–13 m, spacing = 1–6 m, local mud filling, poor combination, belonging to the weak structural plane. LX2: 273°–335°∠83°–88°, opening width = 2–25 cm, extension = 2–6 m, spacing = 1–8 m, local mud filling, combined with general. It has a hard structural plane (LX1 and LX2 represent the two groups of primary fractures developed in bedrock).

FIGURE 3
(A) Crushed stone soil in ZK2. **(B)** Sliding zone soil in ZK3.
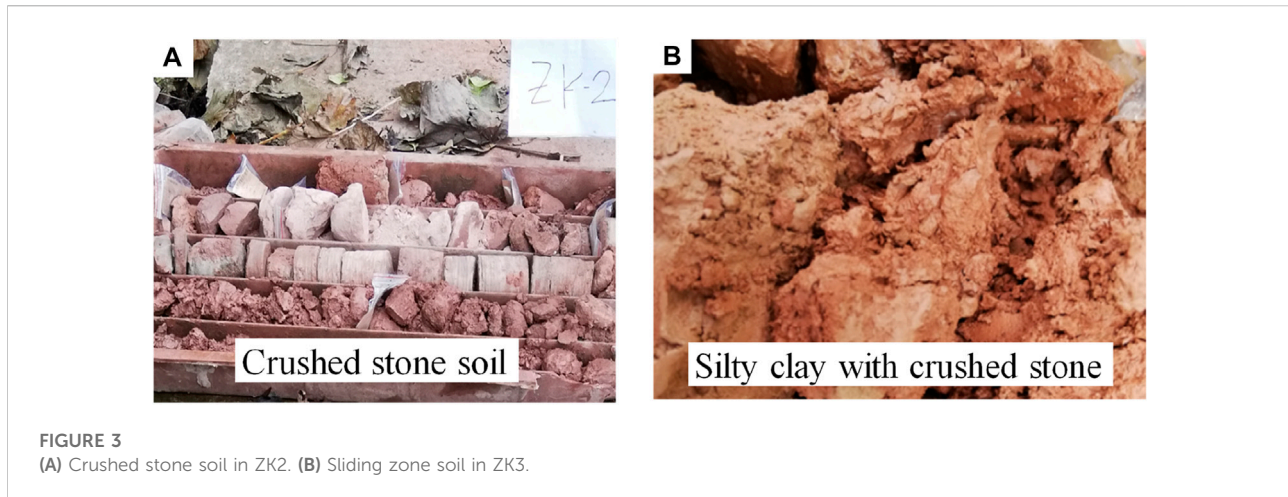
2.1.3 Hydrogeological conditions

The landslide region has a subtropical warm and humid monsoon climate zone with complex topography. Atmospheric rainfall is the primary source of groundwater. The excellent surface water discharge conditions are attributable to the significant terrain height difference in the area and the steep terrain slope. The rain is mostly released directly to the slope toe along the slope surface and cracks, and less water infiltrates into the soil layer. Simultaneously, the soil layer mainly comprises broken stone soil. The uneven distribution of stone, good permeability, and interbedded mudstone and sandstone are some features of the bedrock. The mudstone exhibits a water-blocking effect; therefore, a poor amount of groundwater is found in the landslide area.

2.2 Landslide characteristics

2.2.1 Material composition of landslide

1) Slider. The primary material composition of the sliding mass is the quaternary colluvial layer (Q_4^{col+dl}) broken stone soil (Figure 3A). The crushed rock soil comprises crushed rock and silty clay. The structure is slightly dense and wet. The content of crushed rock is 55%–75%, the particle size is 2–10 cm, and the maximum size is 1.1 m. It is subangular and consists of sandstone and mudstone. Silty clay is brown yellow, purple-brown, and plastic. Its thickness is 6.8–12.9 m.
2) Sliding belt. The drilling process revealed that the sliding zone's thickness was 0.2–0.3 m, mostly comprising brownish-yellow silty clay with gravel (Figure 3B). Its gravel content is 25%–30%, with the particle size of 0.2–4 cm and subangular to subcircular shapes. The gravel composition is sandstone and mudstone and is strongly weathered. The silty clay is in a plastic state.
3) Sliding bed. The sliding bed comprises a broken line along the main sliding direction. With steep upper and slow lower parts, its average inclination angle is about 28°. The trailing edge sliding bed is broken stone soil. The content of the broken stone is 60%–75%, the particle size is generally 2–8 cm, the maximum is about 9.7 m, and the layer thickness is generally 1.5–16.2 m. The front sliding bed is sandstone and mudstone of the Upper Jurassic Penglaizhen Formation (J_3P). The rock stratum is at 350°∠6°, strongly weathered, and has a thickness of 0.7–2.1 m.

2.2.2 Landslide boundary

The plane shape of the landslide has an appearance of a "tongue." The rock and soil steep slopes are present over the trailing edge boundary. The other boundary is the landslide accumulation of block stone soil (Figure 4A). The terrain slope of the leading edge boundary is steep, with primarily exposed lower outer slope body. No evident sign of deformation was present (Figure 4B). The bedrock surface binds the left and right sides of the landslide. There is locally exposed bedrock, thin soil, and no evidence of deformation on the slope on the west side of the left boundary (the east side of the right boundary) (Figure 4C). The slope's soil thickness on the east side of the left boundary (the west side of the right boundary) is relatively large, with the apparent deformation of the slope (Figure 4D).

2.2.3 Landslide deformation characteristics

The deformation trend slowed down in 1982 following substantial deformation, such as tensile cracks in the trailing edge of the landslide. However, a trend of active deformation has been observed in recent years. A local slip occurred at the trailing edge of the landslide in August 2008. From 2015 to 2018, the cracks at the trailing edge of the landslide became large, with an extension length of around 12 m and an opening width of about 5–10 cm. It was filled with silty clay mixed with gravel (Figure 5A). In June 2018, the local collapse occurred in the middle of the landslide. Consequently, the sliding soil interrupted the highway traffic (Figure 5B).
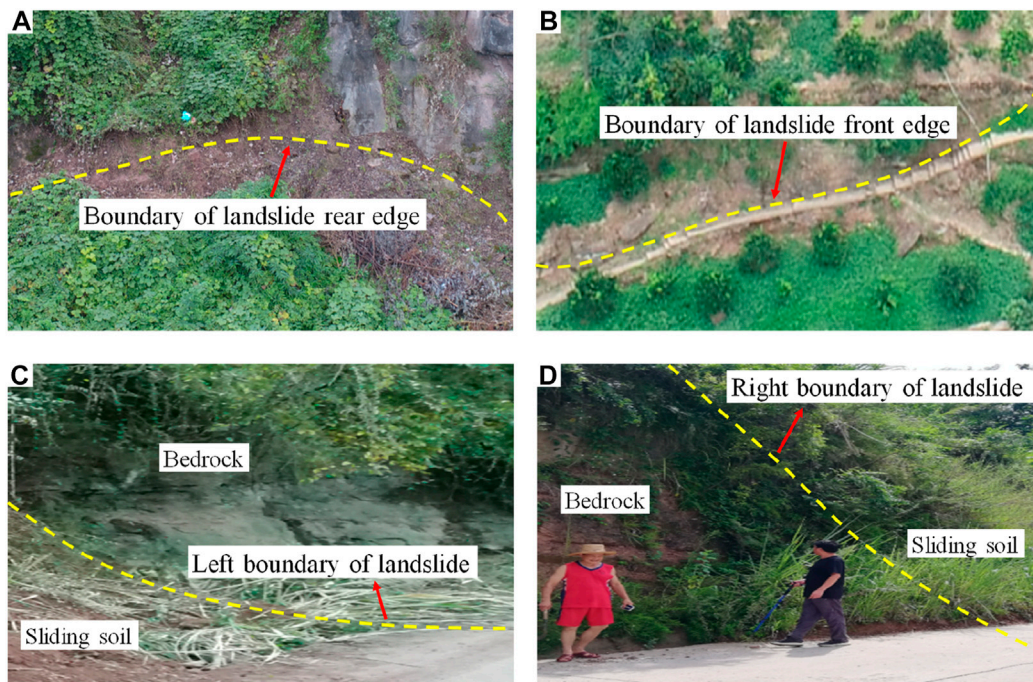
FIGURE 4
Landslide boundary. **(A)** The rear edge of the landslide. **(B)** The front edge of the landslide. **(C)** The left boundary of the landslide. **(D)** The right boundary of the landslide.
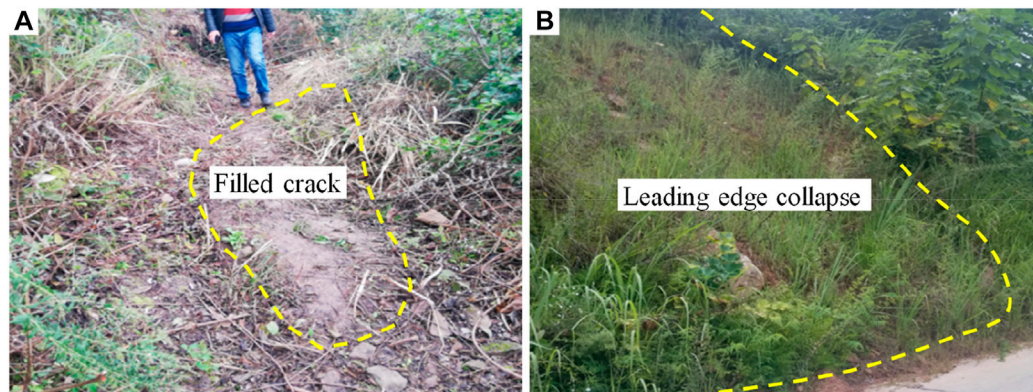
FIGURE 5
Deformation characteristics of landslide. **(A)** Trailing edge crack. **(B)** The local collapse in the middle.

2.3 Influencing factors and formation mechanism of landslides

2.3.1 Influencing factors

The following factors are mainly responsible for the formation of the landslide.

1) Rainfall: The continuous and concentrated rainfall is the main trigger factor for landslides. Heavy rainfall increases the soil weight of the sliding body and reduces the shear strength of the sliding surface, resulting in the deformation and failure of the sliding body.

2) Topography: The landslide area is a low mountain slope landform with structural denudation and erosion. The deeply cut valley, the large terrain height difference, and the steep slope of the front edge of the landslide are the free conditions that cause shear in the landslide.

3) Geological structure and stratum lithology: the landslide region is located in the adaxial part of the southeast wing of the Wanzhou

TABLE 1 Physical and mechanical parameters of rock and soil of Xinjin landslide.

Type	Natural weight (kN/m³)	Saturated weight (kN/m³)	Natural c (kPa)	Natural φ (°)	Saturated c (kPa)	Saturated φ (°)
Gravel soil	20.22	21.21	20	19	18	17
Silty clay with crushed stone	20.00	20.50	18.60	15.50	16.50	13
mudstone	25.10	25.30	265	29.06	150	25
Bedrock	25.20	25.30	980	35.08	650	33

①-Original ground line; 2-Excavate the slope before deformation;
③-A deformed fracture body sliding along the shale interbedded plane.

FIGURE 6
Sliding-cracking landslide failure mode (Zhang et al., 2016).
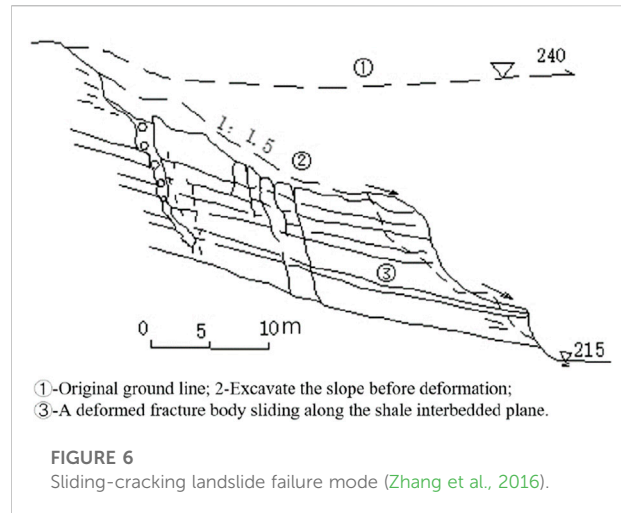
syncline. Some of its characteristics are the monoclinic rock stratum and the prevalent bedrock fissures. The rock stratum tendency is consistent with the slope direction, and the stratum lithology comprises interbedded mudstone and sandstone. Due to differential weathering, it is easy for the rock mass to create a mudstone cavity, leading to the further formation of dangerous rock mass and a large number of accumulation bodies at the foot of the slope. This feature provides structural conditions and material sources for the formation of landslides.

4) Material composition: the landslide mainly consists of broken stone soil with a loose to medium-density structure and good permeability. The infiltration of atmospheric rainfall surface water increases the sliding body's weight. As a result, the mechanical properties of the sliding zone are reduced, thereby decreasing the landslide's stability.

5) Human engineering activities: Figure 1 shows a path in the middle and front of the landslide. The unloading effect of excavation during construction somewhat diminishes the anti-sliding force of the landslide. Simultaneously, agricultural activities of farmers at the rear edge of the landslide also increased the sliding force of the landslide to a certain extent. Together, they both act to lower the landslide's stability.

2.3.2 Formation mechanism

The slope of the terrain in the landslide area ranges from 15° to 40°. The steeper slope of the trailing edge has slower middle and front parts. The overlying soil layer is loose, broken stone soil. The large soil block stone content in the area has a relatively permeable layer. Rainfall infiltration changes the physical and mechanical properties of the shallow soil. The slope is deformed because of gravity. The stress is further concentrated under the accumulation of long-term deformation, leading to sliding.

The steep and gentle changes in the slope's shape create suitable terrain conditions for its slip (Hou et al., 2013). Moreover, the stratum tendency is the same as that of the rock stratum tendency.

FIGURE 7
Schematic diagram of the implicit solution calculation model of the transfer coefficient method for slope with broken line sliding surface (In this paper, the landslide 1−1′ section is divided into nine blocks for overall stability calculation, and the stability of two possible secondary shear outlets is also calculated) (Baker et al., 1980; Hutchinson et al., 1982).
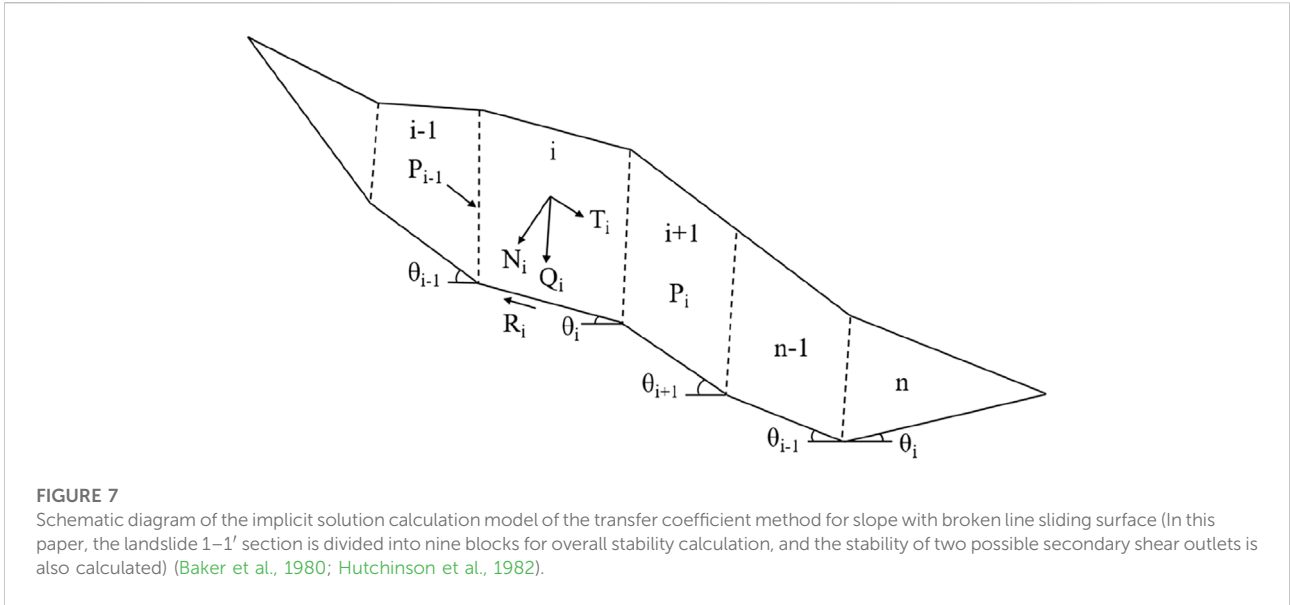
TABLE 2 Stability calculation results of transfer coefficient method.

Working condition	Stability factor	Safety factor	Residual sliding force (kN/m)	Stability determination
Natural working condition	1.212	1.15	0	Stable
Rainstorm condition	1.040	1.15	139.19	Unstable

TABLE 3 Classification of landslide stability.

Stability factor fs	Fs < 1.00	1.00 ≤ Fs < 1.05	1.05 ≤ Fs < Fst	Fs ≥ Fst
stability	instable	Unstable	Basically stable	stable

The landslide section depicts the thin upper rock stratum of the sliding body and the delicate lower part. Moreover, tensile cracks are present at the trailing edge of the landslide. The landslide has a medium dip angle. When it rains heavily, the surface water penetrates downward. The water flow is concentrated in the weak rock at the bottom of the landslide, thus accelerating the softening of the soft rock, reducing the bearing capacity of the rock, and then causing sliding. Therefore, the landslide conforms to the sliding-cracking failure mode (Figure 6).

3 Landslide stability analysis

3.1 Calculation model and calculation method

Because the leading edge of the landslide body does not enter into the water, and there is no steady groundwater level during the exploration period, the effects of pore water static pressure and

hydrodynamic pressure are not considered in the calculation (Liu and Yin, 2003; Troncone et al., 2020). The potential sliding surface of the landslide is undulating and uneven. The implicit solution (broken line sliding surface) of the transfer coefficient method is applied to calculate the landslide's stability. The calculation model (Figure 7) and formula are presented as follows.

Calculation method:

$$P_n = 0 \tag{1}$$

$$P_i = P_{i-1}\psi_{i-1} + T_i - R_i/F_s \tag{2}$$

$$\psi_{i-1} = \cos(\theta_{i-1} - \theta_i) - \sin(\theta_{i-1} - \theta_i)\tan\varphi_i/F_s \tag{3}$$

$$T_i = (G_i + G_{bi})\sin\theta_i + Q_i\cos\theta_i \tag{4}$$

$$R_i = c_i l_i + [(G_i + G_{bi})\cos\theta_i - Q_i\sin\theta_i - U_i]\tan\varphi_i \tag{5}$$

where P_n is the residual slide force per unit width of the nth block; P_i is the residual sliding force per unit width of the i calculation block and the $i + 1$ calculation block. When $P_i < 0$ ($i < n$), $P_i = 0$. T_i is the unit width gravity of the ith slice and the sliding force caused by other external forces; R_i first calculates the anti-sliding force caused by the unit width

FIGURE 8
Simulation results of stability. **(A)** Morgenstern-Price natural state. **(B)** Morgenstern-Price rainstorm status. **(C)** Bishop natural state. **(D)** Bishop rainstorm status. **(E)** Janbu natural state. **(F)** Janbu rainstorm status.
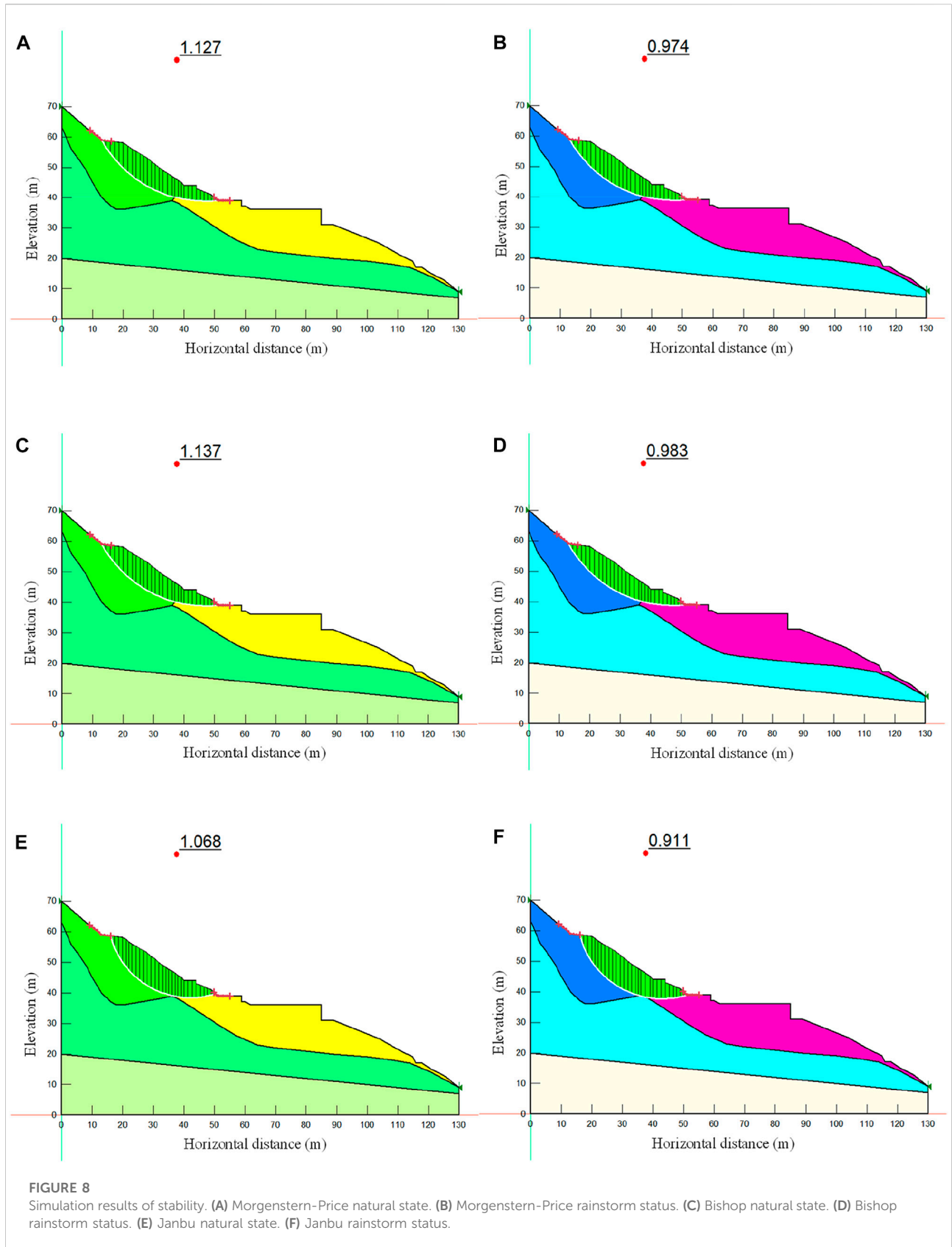
Method	Morgenstern-price	Bishop	Janbu	Stability discrimination
Natural working condition	1.128	1.137	1.061	Basically stable
Rainstorm working condition	0.974	0.984	0.916	Instable

gravity and other external forces; Ψ_{i-1} calculates the transfer coefficient of the block for the $i-1$ to the i; φ_i calculates the internal friction angle of the slice soil for the ith; c_i is the cohesion of the ith calculated slice soil; l_i is the length of sliding surface of the ith calculated slice; G_i is the weight per unit width of the slipping mass calculated for the first i; G_{bi} is the unit width additional load of the ith slice slider; θ_i is the first i to calculate the dip angle of the slip surface of the strip; Q_i is the horizontal load per unit width of the ith calculated slider; U_i is the unit total water pressure of the ith calculated sliding block; and Fs is the safety factor.

3.2 Calculation conditions and parameter selection

The earthquake's effects are not considered because of the location of the landslide area (Du et al., 2015; Mi and Wang, 2021). Rainfall is one of the fundamental reasons for the instability of unsaturated soil (Feng et al., 2013; Liu et al., 2018). A large amount of rainwater penetrates the slope soil, thus altering the mechanical properties of the slope soil and causing instability in the slope. Therefore, the following two conditions are used to calculate the landslide's stability. The safety factor is 1.15 according to the interpolation method. A safety factor is the ratio of anti-sliding force and sliding force on the sliding surface, which is the crucial index to evaluate the landslide's stability. The safety factor is greater than 1, indicating that the landslide is stable. The larger the value, the smaller the possibility of sliding. A safety factor of less than 1 suggests that the landslide is unstable. The smaller the value, the greater the possibility of sliding.

Natural conditions: self-weight + surface load; it is regarded as the full saturation state below the groundwater level, and the other is the natural state.

Rainstorm conditions: weight + surface load + rainstorm; the landslide body is the state of full saturation.

Table 1 shows the parameters selected according to the geotechnical test results and engineering experience.

3.3 Calculation results

Table 2 presents the calculation results of landslide stability.

According to the calculation results and the landslide stability classification table (Table 3), the landslide is stable under natural conditions and unstable under rainstorm conditions.

4 Numerical simulation analysis

4.1 Simulation software

The GeoStudio software developed by the GeoSlope Company of Canada is used in this simulation. This software includes the following eight modules: SLOPE/W, SEEP/W, SIGMA/W, QUAKE/W, TEMP/W, CTRAN/W, AIR/W, and VADOSE/W. The analysis results of each module are interchangeable. The SLOPE/W module built in the GeoStudio software applies the limit equilibrium theory to analyze the stability of slopes with different soil types, complex strata, and slip surface shapes, which can directly obtain the safety factor of slopes. Alternative limit equilibrium methods include Morgenstern-Price, Bishop, Janbu, Sarma, GLE, Spencer, among others. Morgenstern-Price, Bishop, and Janbu are used for simulation in this paper.

4.2 Model establishment

The simulation does not consider groundwater's effects on the landslide's stability. The section having a length of 130 m and a height of 70 m is selected as the calculation model. According to the different lithologies, the slope is divided into four areas: broken stone soil, silty clay with gravel, mudstone, and bedrock. It is assumed that the constitutive relationship between the stress and strain of slope rock mass is elastic-plastic. The failure of rock mass follows the Mohr-Coulomb criterion. The horizontal and vertical axes are selected as the stress and deformation boundaries of the model.

The simulation steps are as follows. Firstly, according to the landslide profile, the software automatically creates a closed graph *via* the input plane coordinates, namely the landslide model outline, to determine the plane coordinates of the feature points. Second, the landslide contour map is divided into four different material areas by coordinate inputs, namely broken stone soil, silty clay with gravel, mudstone, and bedrock, according to the plane characteristics of the landslide body, the sliding zone and the sliding bed of the landslide, and the lithology of the stratum. Next, the parameters of the four material areas, gravity, cohesion, and internal friction angle, are input. Finally, the landslide model can be calculated by selecting the entry and exit parts of the landslide to obtain the most dangerous sliding surface position of the landslide and its corresponding safety factors.

FIGURE 9
Numerical simulation results after treatment (The black line crossing the stratum in the figure represents the anti-slide pile set). **(A)** Morgenstern-Price. **(B)** Bishop. **(C)** Janbu.
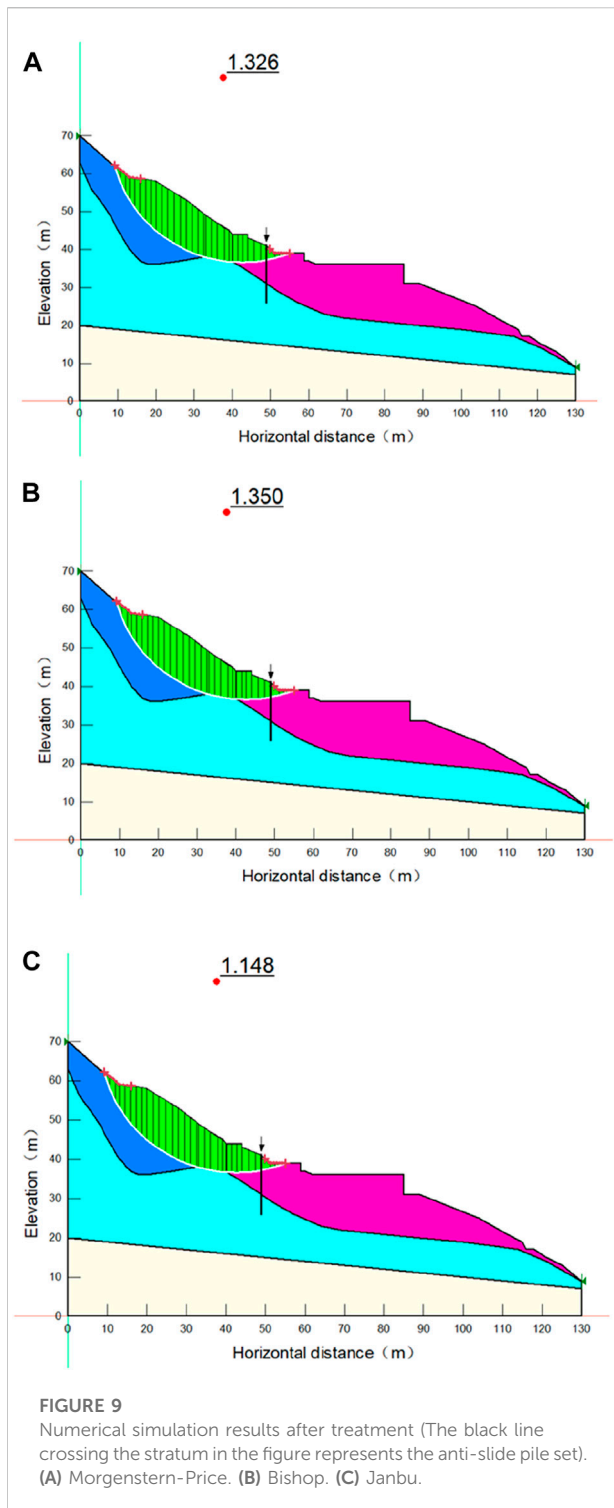
4.3 Calculation conditions and parameter selection

The simulation is conducted under two working conditions (the natural state and the rainstorm state). The stability safety

factor is 1.15. The selection of calculation parameters is determined by indoor soil test results and engineering experience (Table 1).

4.4 Simulation results

Figure 8 depicts the simulation results of the three methods, and Table 4 presents the verification results.

The numerical simulation results demonstrate that the stability coefficients obtained under rainstorm conditions are smaller than those obtained under natural conditions. Under the same conditions, the stability coefficient obtained by the Bishop method is the largest, followed by the Morgenstern-Price method and the Janbu method. According to the simulation results and Table 3, the landslide is basically stable under natural conditions and unstable under rainstorm conditions.

4.5 Comprehensive evaluation of stability

The calculation results of the transfer coefficient method illustrate that the landslide is in a stable state under natural conditions and in an unstable state under rainstorm conditions. The numerical simulation results depict that the landslide is basically stable under natural conditions and unstable under heavy rain conditions. The limit equilibrium method in the numerical simulation adopts the slice method in the analysis and calculation; this reason accounts for the difference between these two outcomes. The slice method does not consider the force between the slices, which may cause some errors and generate fewer results. Based on the findings of the above two approaches, the landslide is in a stable state under natural conditions and in an unstable state under rainstorm conditions.

The investigation of the landslide reveals that the landslide has no apparent deformation during the dry season. Moreover, evident signs of deformation are visible in the middle and rear parts of the landslide during the rainstorm. The current situation is in a stable state. Under adverse conditions, such as heavy rainfall, the landslide is in an unstable state as a whole, with a possibility of overall shear slip (Han et al., 2019; Ogbonnaya and Chidinma, 2019). In summary, the landslide stability calculation results are basically consistent with the actual stable state.

4.6 Preventive measures

4.6.1 Drainage works

According to the above analysis, the landslide is unstable under rainstorm conditions. A perfect surface and underground drainage system must be installed on the landslide's location to address the stability problem of the landslide, ensure the smooth

TABLE 5 Comparison of simulation results before and after treatment.

Governance states	Morgenstern-price	Bishop	Janbu	Stability discrimination
Before governance	0.974	0.983	0.911	unstable
After governance	1.326	1.350	1.148	stable
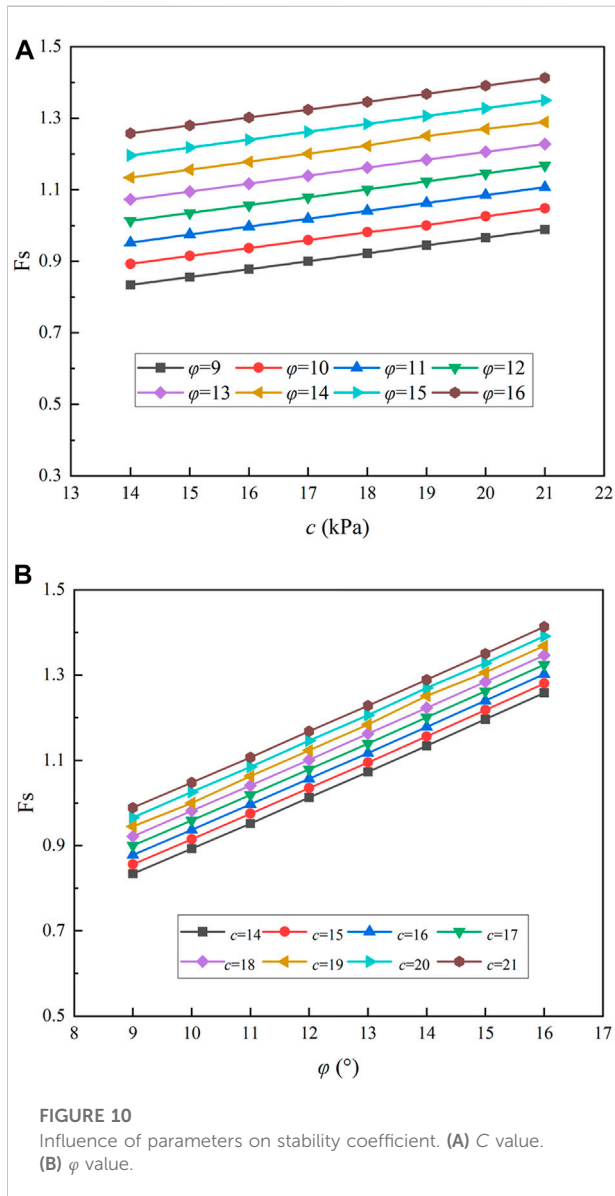
FIGURE 10
Influence of parameters on stability coefficient. **(A)** C value. **(B)** φ value.

4.6.2 Retaining works

A gravity-retaining wall with a length of about 43 m, a height of about 7 m, and an area of about 300 m² is constructed on the landslide; this wall enhances the landslide's stability to a certain extent. Anti-slide piles are installed at the front edge of the landslide according to the terrain, vegetation, and construction conditions of the landslide. Cast-in-situ retaining plates are used between the piles to stabilize the landslide under rainstorm conditions. The length of the anti-slide bank is about 15 m, the pile section size is 1.5 m × 2.0 m, the pile spacing is 3 m, and the pile shaft concrete is C30.

4.6.3 Simulation after treatment

The 1–1' section of the landslide is taken as the research objective, and the reinforcement load is selected as the anti-slide pile. Sections 3.1 and 3.2 provide details on the selection of simulation steps and parameters. Three different methods are used to conduct numerical simulations under rainstorm conditions. Figure 9 shows the simulation results.

The comparison between Figures 8, 9 shows that the safety factor of the landslide has altered before and after the treatment (Table 5).

Table 5 shows that under the rainstorm condition, the safety factors of the landslide before treatment are less than 1, and the landslide is in an unstable state. Following treatment, the safety factor of the landslide is increased. In addition, the average safety factor obtained by the three methods is more than 1.15, indicating that the landslide is in a stable state and that the prevention and control measures have effectively increased the landslide's stability.

5 Discussions

The shear strength of soil can be divided into two parts. One is related to the normal stress between particles, whose essence is friction. The other part that does not depend on normal stress is called cohesion. When the shear stress generated by the external load reaches the shear strength of the soil, the soil is destroyed. In severe cases, a landslide will occur. The soil lithology of the Xinjinxiang landslide sliding zone is silty clay mixed with gravel, and the gravel with limited content plays a vital role in stability. This paper selected the 1–1' section of the landslide to slide as a whole and conducted the sensitivity analysis of shear strength

release of water, and reduce the adverse rainfall effects on the landslide's stability. In the preliminary design, a 100-m long longitudinal drainage ditch is arranged based on the existing gullies on the landslide, which is connected with the village's drainage system to expedite the surface water drainage.

under a rainstorm to investigate the effects of landslide stability on the sensitivity of shear strength parameters (Figure 10).

The results show an apparent linear relationship among c, φ, and the stability coefficient. The stability of an unstable slope is more sensitive to the φ value than the c value. The reason for this outcome is that the sliding mass of the landslide mainly comprises silty clay with crushed stone, wherein the crushed stone accounts for a large proportion, resulting in a low binding force between particles. Hence, the landslide's stability is not significantly affected by the value of c. Analyzing the sensitivity of shear strength parameters to slope safety factors can guide the selection of soil slope rock mass parameters and provide a foundation for selecting landslide prevention measures.

6 Conclusion

1) The plane shape of the landslide has a tongue-shaped appearance. The bedrock surface bounds the left and right sides, and obvious deformation signs can be seen at the boundary. The trailing edge is bounded by the rock steep slope and the soil steep slope, and the rock steep slope binds the leading edge. The volume is about $1.7\,m^3 \times 10^4\,m^3$, which signifies a small middle-level soil landslide. The landslide formation results from the interaction of topography, geological structure, lithology, and rainfall. According to the field investigation and analysis, the failure mode of the landslide is determined to be a slip crack.

2) The calculation results of the transfer coefficient method demonstrate that the landslide is in a stable state under natural conditions. In contrast, the landslide is in an unstable state under rainstorm conditions.

3) The numerical simulation results illustrate that the landslide is stable under natural and unstable under rainstorm conditions. Under the same conditions, the Bishop method has the largest value of the stability coefficient, followed by the Morgenstern-Price method, with the second highest value, and the Janbu method, with the smallest value of the stability coefficient.

4) Compared with the transfer coefficient method, the stability coefficient obtained by numerical simulation is smaller. Combining the results of the two methods revealed that the landslide is in a stable state under natural conditions and in an unstable state under rainstorm conditions.

5) The stability coefficient of the landslide is improved following the installation of the anti-slide pile and retaining wall. Notably, the unstable state becomes stable under rainstorm conditions, indicating that the control measures have improved the landslide's stability. Such prevention and control measures can also be implemented for similar small rock slopes.

6) The shear strength sensitivity analysis of the landslide profile under rainstorm conditions shows a clear linear relationship among c, φ, and stability coefficient, and the stability of unstable slope is more sensitive to φ than to c.

Data availability statement

The raw data supporting the conclusions of this article will be made available by the authors, without undue reservation.

Author contributions

All authors listed have made a substantial, direct, and intellectual contribution to the work and approved it for publication.

Conflict of interest

Author YG was employed by PowerChina Huadong Engineering Corporation Limited. Author JJ was employed by Chongqing 208 Geological Environment Research Institute Co., Ltd.

The remaining authors declare that the research was conducted in the absence of any commercial or financial relationships that could be construed as a potential conflict of interest.

Publisher's note

All claims expressed in this article are solely those of the authors and do not necessarily represent those of their affiliated organizations, or those of the publisher, the editors and the reviewers. Any product that may be evaluated in this article, or claim that may be made by its manufacturer, is not guaranteed or endorsed by the publisher.

References

Baker, R. (1980). Determination of the critical slip surface in slope stability computations. *Int. J. Numer. Anal. Methods Geomech.* 4 (4), 333–359. doi:10.1002/nag.1610040405

Chen, X. P., Zhu, H. H., Huang, J. W., and Liu, D. (2016). Stability analysis of an ancient landslide considering shear strength reduction behavior of slip zone soil. *Landslides* 13 (1), 173–181. doi:10.1007/s10346-015-0629-7

Cheng, X. Z., Tang, H. M., Yang, Y. C., Hu, B., and Ni, J. (2008). 3D analysis of landslide stability based on strength reduction FLAC~3D: Taking baigunshu paleo-landslide group in the three Gorges reservoir area as an example. *Hydrogeology Eng. Geol.* 2008(2), 24–28. doi:10.1016/S1876-3804(08)60015-4

Du, F., Ren, G. M., Xia, M., Gao, B., Yu, T. B., and Wu, L. K. (2015). Numerical simulation of recurrence mechanism of old landslide under earthquake loading. *Mt. Res.* 33 (2), 233–239. doi:10.16089/j.cnki.1008-2786.000030

Duncan, J. M. (1996). State of the art: Limit equilibrium and finite-element analysis of slopes. *J. Geotech. Engrg.* 122 (7), 577–596. doi:10.1061/(asce)0733-9410(1996)122:7(577)

Fan, R. L., Zhang, L. M., and Shen, P. (2019). Evaluating volume of coseismic landslide clusters by flow direction-based partitioning. *Eng. Geol.* 260, 105238. doi:10.1016/j.enggeo.2019.105238

Feng, W., Wang, J. Y., Zhang, C. H., and Gaq, B. (2013). Analysis on the influence of the rainfall infiltration on the stability of qiujialiang landslide. *Northwest. Geol.* 46 (2), 195–200. doi:10.3969/j.issn.1009-6248.2013.02.024

Gong, W. P., Juang, C. H., and Wasowski, J. (2021). Geohazards and human settlements: Lessons learned from multiple relocation events in Badong, China–Engineering geologist's perspective. *Eng. Geol.* 285, 106051. doi:10.1016/j.enggeo.2021.106051

Guo, M. W., Liu, S. J., Yin, S. D., and Wang, S. L. (2019). Stability analysis of the Zhangmu multi-layer landslide using the vector sum method in Tibet, China. *Bull. Eng. Geol. Environ.* 78 (6), 4187–4200. doi:10.1007/s10064-018-1386-3

Han, Z., Su, B., Li, Y. E., Ma, Y. F., Wang, W. D., and Chen, G. Q. (2019). Comprehensive analysis of landslide stability and related countermeasures: A case study of the lanmuxi landslide in China. *Sci. Rep.* 9 (1), 12407–12412. doi:10.1038/s41598-019-48934-3

Hou, T. S., Xu, G. L., Shen, Y. J., Wu, Z. Z., Zhang, N. N., and Wang, R. (2013). Formation mechanism and stability analysis of the Houba expansive soil landslide. *Eng. Geol.* 161, 34–43. doi:10.1016/j.enggeo.2013.04.010

Hutchinson, J. N. (1982). *Methods of locating slip surface in landslides*. London, UK: British Geomorphological Research Group.

Li, A., Dai, F., Liu, Y., Liu, K., and Wang, K. (2022). Deformation characteristics of sidewall and anchorage mechanisms of prestressed cables in layered rock strata dipping steeply into the inner space of underground powerhouse cavern. *Int. J. Rock Mech. Min. Sci.* 159, 105234. doi:10.1016/j.ijrmms.2022.105234

Liu, G., Tong, F. G., Zhao, Y. T., and Tian, B. (2018). A force transfer mechanism for triggering landslides during rainfall infiltration. *J. Mt. Sci.* 15 (11), 2480–2491. doi:10.1007/s11629-018-5043-x

Liu, L. L., and Yin, K. L. (2003). Discrete element method applied to stability analysis of landslides along reservoir shoreline. *Hydrogeology Eng. Geol.* 30 (4), 63. doi:10.1007/s11769-003-0044-1

Luo, Y. H., Zhang, Y., Wang, Y. S., He, Y., Zhang, Y. Y., and Cao, H. (2021). A unique failure model for a landslide induced by the Wenchuan earthquake in the Liujiawan area, Qingchuan County, China. *Eng. Geol.* 295, 106412. doi:10.1016/j.enggeo.2021.106412

Ma, Z. Y., Zhu, C. H., Yao, X. L., and Dang, F. N. (2021). Slope stability analysis under complex stress state with saturated and unsaturated seepage flow. *Geofluids* 2021, 1–11. doi:10.1155/2021/6637098

Mi, Y., and Wang, J. H. (2021). Finite-element modeling of submarine landslide triggered by seismic loading in saturated cohesive soil deposits. *Bull. Eng. Geol. Environ.* 80 (2), 951–965. doi:10.1007/s10064-020-02005-4

Ogbonnaya, I., and Chidinma, C. (2019). Slope stability analysis of mine waste dumps at a mine site in Southeastern Nigeria. *Bull. Eng. Geol. Environ.* 78 (4), 2503–2517. doi:10.1007/s10064-018-1304-8

Sarkar, S., Pandit, K., Dahiya, N., and Chandna, P. (2021). Quantified landslide hazard assessment based on finite element slope stability analysis for Uttarkashi–Gangnani Highway in Indian Himalayas. *Nat. Hazards (Dordr).* 106 (3), 1895–1914. doi:10.1007/s11069-021-04518-x

Tang, H. M., Wasowski, J., and Juang, C. H. (2019). Geohazards in the three Gorges reservoir area, China–lessons learned from decades of research. *Eng. Geol.* 261, 105267. doi:10.1016/j.enggeo.2019.105267

Tao, Y. F., Xue, Y. G., Li, S. C., Qiu, D. H., Li, Z. Q., and Zhang, K. (2019). Parameter susceptibility analysis of the shimen landslide (liaoning Province, China). *Soil Mech. Found. Eng.* 56 (1), 7–11. doi:10.1007/s11204-019-09562-1

Troncone, A., Pugliese, L., and Conte, E. (2020). Run-out simulation of a landslide triggered by an increase in the groundwater level using the material point method. *Water* 12 (10), 2817. doi:10.3390/w12102817

Xu, W. J., Hu, R. L., Yue, Z. Q., and Tan, R. J. (2009). Genesis and stability of the zhoujiawan landslide, three Gorges, China. *Bull. Eng. Geol. Environ.* 68 (1), 47–54. doi:10.1007/s10064-008-0154-1

Zhang, Y., Yin, K. L., Guo, Z. Z., Liang, X., Tan, M. J., and Yang, Y. G. (2019). Evaluation of the Stability of Maliulin Landslide under the Reservoir Water Level Fluctuation Combined with Rainfall. *Geol. Sci. Tech. Inf.* 38 (6), 198–205. doi:10.19509/j.cnki.dzkq.2019.0623

Zhang, Z. Y., Wang, L. S., and Wang, S. T. (2016). *Principles of Engineering Geological Analysis*. 4th Edn. Beijing: Geological Publishing House.

Zhao, L. H., Liu, X. N., Mao, J., Shao, L. Y., and Li, T. C. (2020). Three-dimensional distance potential discrete element method for the numerical simulation of landslides. *Landslides* 17 (2), 361–377. doi:10.1007/s10346-019-01282-9

Zhou, J. W., Xu, W. Y., Yang, X. G., Shi, C., and Yang, Z. H. (2010). The 28 october 1996 landslide and analysis of the stability of the current huashiban slope at the liangjiaren hydropower station, southwest China. *Eng. Geol.* 114 (1-2), 45–56. doi:10.1016/j.enggeo.2010.04.001

Zhou, X. P., Zhu, B. Z., and Wong, L. N. Y. (2019). A stability analysis of landslides based on random fields-Part I: Toe circle slope. *Bull. Eng. Geol. Environ.* 78 (1), 103–115.